

Supporting Information for:

The Mechanism of the Hydrophobic Effect in the
Biomolecular Recognition of Arylsulfonamides by Carbonic
Anhydrase

Phillip W. Snyder^a, Jasmin Mecinović^a, Demetri T. Moustakas^a, Samuel W. Thomas III^a,
Michael Harder^a, Eric T. Mack^a, Matthew R. Lockett^a, Annie Héroux^b, Woody Sherman^c,
George M. Whitesides^{a,d*}

^a*Department of Chemistry and Chemical Biology, Harvard University
12 Oxford Street, Cambridge, MA 02138*

^b*National Synchrotron Light Source, Brookhaven National Laboratory,
725 Brookhaven Avenue, Upton, NY 11973-5000*

^c*Schrodinger, Inc., 120 West 45th Street, New York, NY 10036-4041*

^d*Wyss Institute of Biologically Inspired Engineering, Harvard University,
60 Oxford Street, Cambridge, MA 02138, USA*

*Author to whom correspondence should be addressed

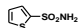
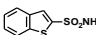
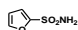
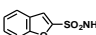
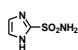
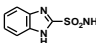
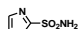
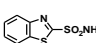
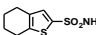
Table of Contents:

| | |
|------|---|
| S3. | Purification of HCA |
| S3. | Isothermal Titration Calorimetry |
| S4. | Table S1. Average Observed Thermodynamic Parameters for the Binding of Sulfonamides to HCA |
| S5. | Table S2. Observed ITC Data for the Individual Titrations |
| S7. | Measurement of the pK_a of the Sulfonamide Group of the Ligands |
| S8. | Figure S1. Representative Data for the Measurement of the pK_a of a Sulfonamide Group |
| S8. | Correction of the Observed Dissociation Thermodynamics for Differences of pK_a of the Ligands |
| S11. | Table S3. Thermodynamic Binding Parameters for the Binding of Ar-SO ₂ NH ⁻ to HCA |
| S12. | Measurement of ΔG°_{ow} and ΔH°_{ow} of the Ligands |
| S14. | Figure S2. Representative Data for Estimating ΔH°_{ow} by Solution Calorimetry |
| S15. | Correction of the Partitioning Thermodynamic Parameters for Ionization of the Sulfonamide |
| S17. | Estimation of the Thermodynamic Parameters for the Benzo Group |
| S18. | Protein Crystallization |
| S18. | Ligand Soaking Experiments |
| S18. | X-ray Crystallography |
| S19. | Solution of the Crystal Structures |
| S20. | Table S4. Crystallography Data |
| S21. | Figure S3. Crystallographically Defined Molecules of Water in the Binding Pocket of HCA with Ligands |
| S24. | WaterMap Calculations |
| S25. | Table S5. WaterMap Results |
| S25. | References |

Purification of HCA. Native HCA was overexpressed in *E. coli* that had been transformed with the pACA plasmid (a kind gift from Fierke and coworkers) containing the gene for the protein under promotion of the Lac operon (1). Pure protein was prepared following the procedure of Fierke and coworkers (2).

Isothermal Titration Calorimetry. All ITC experiments were conducted on standard volume (1 – 1.5 mL) isothermal titration calorimeters (Nano-SV, TA Instruments ; Auto VP-ITC, GE Healthcare). Stocks solutions of the sulfonamide ligands were prepared in DMSO-*d*₆ at concentrations that gave appropriate concentrations of titrant when diluted (2 μ L) into buffer (1.998 mL). Concentrations of the stock solutions of the ligands were measured using ¹H NMR (3). The buffer for all experiments was sodium phosphate (10 mM, pH = 7.60 \pm 0.03). Titrations comprised 10 – 20 injections (15 – 28 μ L) of ligand (monocyclic compounds, 100 – 500 μ M; bicyclic compounds, 50 – 100 μ M) from the syringe into solutions of HCA that were at 1/12th to 1/20th the concentration of the solution in the syringe(4). The raw data were analyzed using commercial software (NanoAnalyze, TA Instruments; Origin , MicroCal LLC). Nonlinear curve fitting, using a model of single site binding, estimates the association constant and the enthalpy of binding, which were used to estimate the free energy and entropy of binding (Table S1) (5). Values of each thermodynamic parameter represent the average of 7 – 10 experiments and the uncertainties represented are one standard deviation.

Table S1. Average observed thermodynamic parameters for the binding of sulfonamides to HCA^a

| sym | Compound | K_d^{obs} (nM) | $\Delta G^{\circ}_{\text{obs}}$ (kcal mol ⁻¹) | $\Delta H^{\circ}_{\text{obs}}$ (kcal mol ⁻¹) | $-T\Delta S^{\circ}_{\text{obs}}$ (kcal mol ⁻¹) |
|------------|---|----------------------------|--|--|--|
| T |  | 340 ± 10 | -8.81 ± 0.02 | -9.31 ± 0.08 | 0.50 ± 0.09 |
| BT |  | 4 ± 1 | -11.5 ± 0.2 | -12.5 ± 0.4 | 1.0 ± 0.4 |
| F |  | 150 ± 6 | -9.3 ± 0.03 | -13.6 ± 0.4 | 4.3 ± 0.4 |
| BF |  | 2.3 ± 0.4 | -11.8 ± 0.1 | -15.5 ± 0.4 | 3.7 ± 0.3 |
| I |  | 9000 ± 2000 | -6.9 ± 0.2 | -3.7 ± 0.4 | -3.2 ± 0.4 |
| BI |  | 400 ± 30 | -8.64 ± 0.04 | -8.7 ± 0.1 | 0.1 ± 0.1 |
| TA |  | 61 ± 5 | -9.83 ± 0.04 | -12.27 ± 0.07 | 2.44 ± 0.08 |
| BTA |  | 2 ± 1 | -12.0 ± 0.4 | -16.0 ± 0.5 | 4.0 ± 0.6 |
| HBT |  | 19 ± 3 | -10.5 ± 0.09 | -11.6 ± 0.1 | 1.1 ± 0.02 |

^aErrors represent the standard deviation of 7-10 independent ITC measurements.

Table S2. Observed Thermodynamic Parameters for the individual titrations.

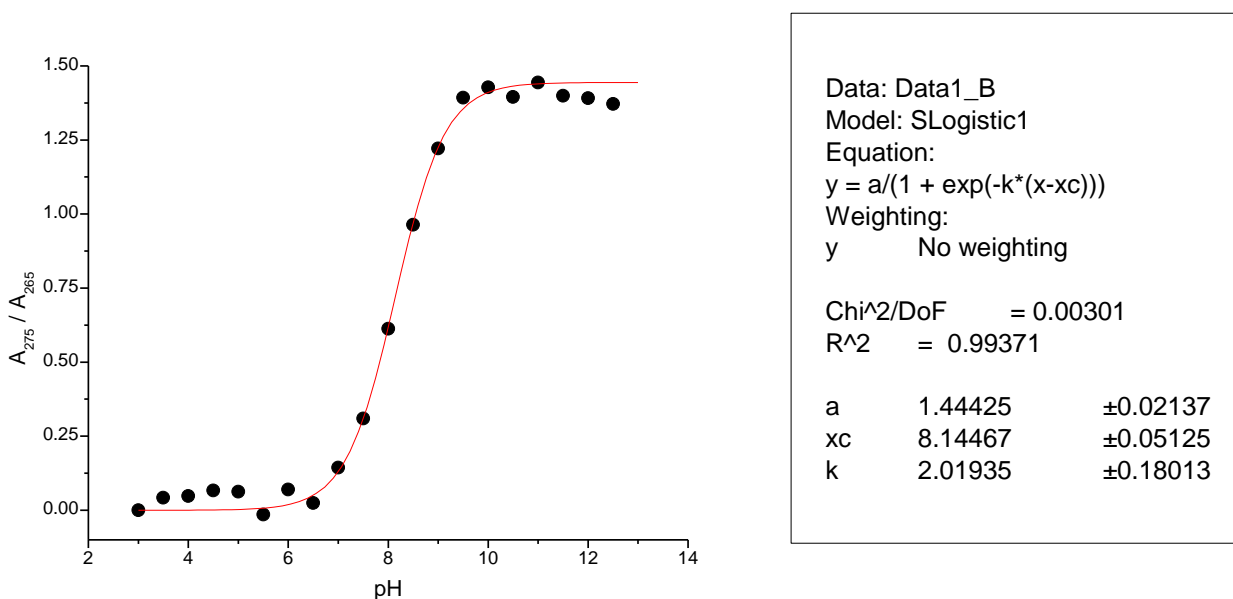
| TA | | | | | | | |
|---------------------|------|--------------------------|---|-----------|---|--|--|
| χ^2/DOF | N | K_a (M ⁻¹) | $\Delta H^\circ_{\text{obs}}$ (kcal mol ⁻¹) | K_d (M) | $\Delta G^\circ_{\text{obs}}$ (kcal mol ⁻¹) | $-\text{TAS}^\circ_{\text{obs}}$ (kcal mol ⁻¹) | |
| 391 | 0.98 | 1.64E+07 | -12.42 | 6.10E-08 | -9.84E+00 | 2.58E+00 | |
| 324 | 0.98 | 1.73E+07 | -12.31 | 5.78E-08 | -9.87E+00 | 2.44E+00 | |
| 413 | 0.98 | 1.65E+07 | -12.25 | 6.06E-08 | -9.84E+00 | 2.41E+00 | |
| 257 | 0.99 | 1.77E+07 | -12.29 | 5.65E-08 | -9.88E+00 | 2.41E+00 | |
| 404 | 0.98 | 1.67E+07 | -12.24 | 5.99E-08 | -9.85E+00 | 2.39E+00 | |
| 981 | 0.99 | 1.46E+07 | -12.26 | 6.85E-08 | -9.77E+00 | 2.49E+00 | |
| 405 | 0.99 | 1.71E+07 | -12.18 | 5.85E-08 | -9.86E+00 | 2.32E+00 | |
| 703 | 0.99 | 1.71E+07 | -12.22 | 5.85E-08 | -9.86E+00 | 2.36E+00 | |
| 918 | 0.98 | 1.45E+07 | -12.23 | 6.90E-08 | -9.76E+00 | 2.47E+00 | |
| 1156 | 0.98 | 1.51E+07 | -12.33 | 6.62E-08 | -9.79E+00 | 2.54E+00 | |
| BTA | | | | | | | |
| χ^2/DOF | N | K_a (M ⁻¹) | $\Delta H^\circ_{\text{obs}}$ (kcal mol ⁻¹) | K_d (M) | $\Delta G^\circ_{\text{obs}}$ (kcal mol ⁻¹) | $-\text{TAS}^\circ_{\text{obs}}$ (kcal mol ⁻¹) | |
| 5894 | 1.00 | 4.38E+08 | -16.02 | 2.28E-09 | -1.18E+01 | 4.24E+00 | |
| 4171 | 1.00 | 4.21E+08 | -15.85 | 2.38E-09 | -1.18E+01 | 4.09E+00 | |
| 14820 | 1.00 | 3.99E+08 | -15.99 | 2.51E-09 | -1.17E+01 | 4.26E+00 | |
| 14360 | 1.01 | 4.39E+08 | -15.89 | 2.28E-09 | -1.18E+01 | 4.11E+00 | |
| 5610 | 1.01 | 5.14E+08 | -16.17 | 1.95E-09 | -1.19E+01 | 4.29E+00 | |
| 102700 | 1.03 | 3.09E+09 | -15.3 | 3.24E-10 | -1.29E+01 | 2.36E+00 | |
| 56680 | 1.00 | 1.89E+08 | -17.35 | 5.29E-09 | -1.13E+01 | 6.07E+00 | |
| 1192 | 1.01 | 6.07E+08 | -15.59 | 1.65E-09 | -1.20E+01 | 3.61E+00 | |
| 2605 | 1.00 | 6.66E+08 | -15.93 | 1.50E-09 | -1.20E+01 | 3.90E+00 | |
| 253500 | 1.00 | 1.48E+09 | -15.65 | 6.76E-10 | -1.25E+01 | 3.15E+00 | |
| I | | | | | | | |
| χ^2/DOF | N | K_a (M ⁻¹) | $\Delta H^\circ_{\text{obs}}$ (kcal mol ⁻¹) | K_d (M) | $\Delta G^\circ_{\text{obs}}$ (kcal mol ⁻¹) | $-\text{TAS}^\circ_{\text{obs}}$ (kcal mol ⁻¹) | |
| 21050 | 0.90 | 1.71E+05 | -3.67 | 5.85E-06 | -7.14 | -3.47 | |
| 46360 | 0.93 | 9.01E+04 | -4.14 | 1.11E-05 | -6.76 | -2.62 | |
| 17090 | 1.00 | 1.22E+05 | -3.68 | 8.20E-06 | -6.94 | -3.26 | |
| 22300 | 0.96 | 1.09E+05 | -3.42 | 9.17E-06 | -6.87 | -3.45 | |
| 18150 | 0.90 | 8.60E+04 | -3.94 | 1.16E-05 | -6.73 | -2.79 | |
| 21350 | 0.96 | 8.11E+04 | -3.28 | 1.23E-05 | -6.70 | -3.42 | |
| 38910 | 0.95 | 1.05E+05 | -2.97 | 9.52E-06 | -6.85 | -3.88 | |
| 21050 | 0.90 | 1.71E+05 | -3.67 | 5.85E-06 | -7.14 | -3.47 | |
| 46360 | 0.93 | 9.01E+04 | -4.14 | 1.11E-05 | -6.76 | -2.62 | |
| BI | | | | | | | |
| χ^2/DOF | N | K_a (M ⁻¹) | $\Delta H^\circ_{\text{obs}}$ (kcal mol ⁻¹) | K_d (M) | $\Delta G^\circ_{\text{obs}}$ (kcal mol ⁻¹) | $-\text{TAS}^\circ_{\text{obs}}$ (kcal mol ⁻¹) | |
| 51800 | 0.97 | 2.55E+06 | -8.73 | 3.92E-07 | -8.65 | 0.08 | |
| 166300 | 0.93 | 2.74E+06 | -8.78 | 3.65E-07 | -8.69 | 0.09 | |
| 30410 | 0.96 | 2.73E+06 | -8.76 | 3.66E-07 | -8.69 | 0.07 | |
| 30920 | 0.97 | 2.48E+06 | -8.75 | 4.03E-07 | -8.64 | 0.11 | |
| 44700 | 0.96 | 2.37E+06 | -8.76 | 4.22E-07 | -8.61 | 0.15 | |
| 26940 | 0.96 | 2.26E+06 | -8.85 | 4.42E-07 | -8.58 | 0.27 | |
| 26110 | 0.98 | 2.30E+06 | -8.5 | 4.35E-07 | -8.59 | -0.09 | |
| 36240 | 0.98 | 2.44E+06 | -8.47 | 4.10E-07 | -8.63 | -0.16 | |

| F | | | | | | | |
|---------------------|------|--------------------------|---|-----------|---|--|--|
| χ^2/DOF | N | K_a (M ⁻¹) | $\Delta H^\circ_{\text{obs}}$ (kcal mol ⁻¹) | K_d (M) | $\Delta G^\circ_{\text{obs}}$ (kcal mol ⁻¹) | $-\text{TAS}^\circ_{\text{obs}}$ (kcal mol ⁻¹) | |
| 1080 | 0.95 | 7.21E+06 | -13.87 | 1.39E-07 | -9.35E+00 | 4.52E+00 | |
| 1205 | 0.97 | 6.91E+06 | -13.79 | 1.45E-07 | -9.33E+00 | 4.46E+00 | |
| 680 | 1.05 | 6.26E+06 | -12.53 | 1.60E-07 | -9.27E+00 | 3.26E+00 | |
| 860 | 0.96 | 6.43E+06 | -13.86 | 1.56E-07 | -9.28E+00 | 4.58E+00 | |
| 400 | 0.99 | 6.56E+06 | -13.65 | 1.52E-07 | -9.29E+00 | 4.36E+00 | |
| 1356 | 0.99 | 6.76E+06 | -13.6 | 1.48E-07 | -9.31E+00 | 4.29E+00 | |
| 393 | 0.99 | 6.63E+06 | -13.5 | 1.51E-07 | -9.30E+00 | 4.20E+00 | |
| 957 | 0.94 | 6.73E+06 | -13.83 | 1.49E-07 | -9.31E+00 | 4.52E+00 | |
| 614 | 0.99 | 7.00E+06 | -13.6 | 1.43E-07 | -9.33E+00 | 4.27E+00 | |
| BF | | | | | | | |
| χ^2/DOF | N | K_a (M ⁻¹) | $\Delta H^\circ_{\text{obs}}$ (kcal mol ⁻¹) | K_d (M) | $\Delta G^\circ_{\text{obs}}$ (kcal mol ⁻¹) | $-\text{TAS}^\circ_{\text{obs}}$ (kcal mol ⁻¹) | |
| 68240 | 1.02 | 4.19E+08 | -15.39 | 2.39E-09 | -1.18E+01 | 3.63E+00 | |
| 67470 | 0.98 | 3.52E+08 | -15.3 | 2.84E-09 | -1.17E+01 | 3.65E+00 | |
| 37240 | 1.01 | 3.41E+08 | -14.79 | 2.93E-09 | -1.16E+01 | 3.16E+00 | |
| 34750 | 1.04 | 3.98E+08 | -15.12 | 2.51E-09 | -1.17E+01 | 3.39E+00 | |
| 16750 | 0.98 | 5.90E+08 | -15.51 | 1.69E-09 | -1.20E+01 | 3.55E+00 | |
| 74790 | 1.00 | 5.05E+08 | -15.71 | 1.98E-09 | -1.19E+01 | 3.84E+00 | |
| 52700 | 0.95 | 6.00E+08 | -16.09 | 1.67E-09 | -1.20E+01 | 4.12E+00 | |
| 44120 | 0.99 | 5.11E+08 | -16.01 | 1.96E-09 | -1.19E+01 | 4.14E+00 | |
| 42540 | 1.05 | 3.88E+08 | -15.23 | 2.58E-09 | -1.17E+01 | 3.52E+00 | |
| T | | | | | | | |
| χ^2/DOF | N | K_a (M ⁻¹) | $\Delta H^\circ_{\text{obs}}$ (kcal mol ⁻¹) | K_d (M) | $\Delta G^\circ_{\text{obs}}$ (kcal mol ⁻¹) | $-\text{TAS}^\circ_{\text{obs}}$ (kcal mol ⁻¹) | |
| 360 | 0.96 | 3.16E+06 | -9.203 | 3.16E-07 | -8.86E+00 | 3.41E-01 | |
| 148 | 0.94 | 2.90E+06 | -9.495 | 3.45E-07 | -8.81E+00 | 6.84E-01 | |
| 428 | 0.95 | 3.00E+06 | -9.337 | 3.33E-07 | -8.83E+00 | 5.06E-01 | |
| 139.6 | 0.96 | 2.84E+06 | -9.222 | 3.52E-07 | -8.80E+00 | 4.23E-01 | |
| 230.6 | 0.95 | 2.88E+06 | -9.373 | 3.47E-07 | -8.81E+00 | 5.66E-01 | |
| 778 | 0.97 | 2.96E+06 | -9.269 | 3.38E-07 | -8.82E+00 | 4.46E-01 | |
| 251.9 | 0.95 | 3.04E+06 | -9.35 | 3.29E-07 | -8.84E+00 | 5.11E-01 | |
| 85.23 | 0.96 | 2.82E+06 | -9.272 | 3.55E-07 | -8.79E+00 | 4.78E-01 | |
| 154.1 | 0.96 | 2.75E+06 | -9.273 | 3.64E-07 | -8.78E+00 | 4.93E-01 | |
| 368.7 | 0.94 | 2.85E+06 | -9.299 | 3.51E-07 | -8.80E+00 | 4.98E-01 | |
| BT | | | | | | | |
| χ^2/DOF | N | K_a (M ⁻¹) | $\Delta H^\circ_{\text{obs}}$ (kcal mol ⁻¹) | K_d (M) | $\Delta G^\circ_{\text{obs}}$ (kcal mol ⁻¹) | $-\text{TAS}^\circ_{\text{obs}}$ (kcal mol ⁻¹) | |
| 20830 | 1.05 | 1.94E+08 | -12.17 | 5.15E-09 | -1.13E+01 | 8.70E-01 | |
| 12570 | 1.01 | 2.25E+08 | -12.76 | 4.44E-09 | -1.14E+01 | 1.37E+00 | |
| 18870 | 0.98 | 2.97E+08 | -12.96 | 3.37E-09 | -1.16E+01 | 1.41E+00 | |
| 12130 | 1.01 | 2.38E+08 | -13.18 | 4.20E-09 | -1.14E+01 | 1.76E+00 | |
| 20700 | 0.95 | 2.69E+08 | -12.73 | 3.72E-09 | -1.15E+01 | 1.24E+00 | |
| 14890 | 1.04 | 1.40E+08 | -12.36 | 7.14E-09 | -1.11E+01 | 1.25E+00 | |
| 12040 | 1.03 | 3.15E+08 | -12.46 | 3.17E-09 | -1.16E+01 | 8.73E-01 | |
| 9805 | 0.99 | 3.35E+08 | -12.35 | 2.99E-09 | -1.16E+01 | 7.27E-01 | |
| 3346 | 0.98 | 3.13E+08 | -11.81 | 3.19E-09 | -1.16E+01 | 2.27E-01 | |
| 12120 | 1.02 | 3.41E+08 | -12.18 | 2.93E-09 | -1.16E+01 | 5.46E-01 | |

| HBT | χ^2/DOF | N | K_a (M ⁻¹) | $\Delta H^\circ_{\text{obs}}$ (kcal mol ⁻¹) | K_d (M) | $\Delta G^\circ_{\text{obs}}$ (kcal mol ⁻¹) | $-\text{TAS}^\circ_{\text{obs}}$ (kcal mol ⁻¹) |
|-----|---------------------|------|--------------------------|---|-----------|---|--|
| | 70930 | 1.00 | 4.31E+07 | -11.73 | 2.32E-08 | -10.40 | 1.33 |
| | 9096 | 1.04 | 6.49E+07 | -11.65 | 1.54E-08 | -10.64 | 1.01 |
| | 6.71E+06 | 1.04 | 4.40E+07 | -11.59 | 2.27E-08 | -10.41 | 1.18 |
| | 11530 | 1.05 | 5.08E+07 | -11.58 | 1.97E-08 | -10.50 | 1.08 |
| | 1911 | 1.03 | 6.17E+07 | -11.45 | 1.62E-08 | -10.61 | 0.84 |
| | 7838 | 1.03 | 5.59E+07 | -11.54 | 1.79E-08 | -10.55 | 0.99 |
| | 22870 | 1.05 | 4.35E+07 | -11.71 | 2.30E-08 | -10.40 | 1.31 |
| | 16110 | 1.05 | 5.10E+07 | -11.44 | 1.96E-08 | -10.50 | 0.94 |

Measurement of the pK_a of the sulfonamide group of the ligands. To a buffered solution (10 mM) in a cuvette was added a solution of the ligand (20 mM in DMSO). Following each addition, the solution was mixed thoroughly, and the ultraviolet spectrum ($\lambda = 210 - 310$ nm) was collected. Spectra were collected at each value of pH between 1.0 and 13.0 at intervals of 0.5 pH units using appropriate buffers (i.e., buffers that did not absorb light above 220 nm). The absorbance at was recorded at two wavelengths (typically 10 nm above and below the isosbestic point), and the ratio of those absorbances were plotted as a function of pH (Fig. S1). The data were fit using nonlinear curve fitting with the function “SLogistic1” (OriginLabs) to determine the midpoint of the titration, which provided the pK_a of the sulfonamide.

Figure S1. Estimating the values of pKa for the sulfonamide ligands.



Correction of the observed dissociation thermodynamics for differences of pKa of the ligands. In order to compare the monocyclic and bicyclic compounds in a scheme that was independent of pKa, we converted the observed thermodynamic parameters of binding ($\Delta G^\circ_{\text{obs}}$, $\Delta H^\circ_{\text{obs}}$, and $-\Delta S^\circ_{\text{obs}}$) to those describing the dissociation of HCA-Zn²⁺-NHO₂S-Ar to HCA-OH₂⁺ and Ar-SO₂NH⁻. The following derivation of the equations used for that correction also appears in Krishnamurthy *et al.* (6).

The desired dissociation constant ($K_d^{\text{Ar-SO}_2\text{NH}^-}$) is a function of the concentrations at equilibrium of the anion of the sulfonamide [Ar-SO₂NH⁻] and the zinc-bound water form of HCA [HCA-Zn^{II}-OH₂⁺] (Figure 1):

$$K_d^{Ar-SO_2NH^-} = \frac{[Ar-SO_2NH^-][HCA-OH_2^+]}{[Ar-SO_2NH^- - Zn^{2+} - HCA][H_2O]} \quad (1)$$

The concentrations of $Ar-SO_2NH^-$ and $HCA-Zn^{II}-OH_2^+$ are represented as functions of the total concentrations of $Ar-SO_2NH_2$ and HCA as:

$$[Ar-SO_2NH^-] = \theta_{Ar-SO_2NH^-} ([Ar-SO_2NH^-] + [Ar-SO_2NH_2]) \quad (2)$$

and

$$[HCA-OH_2^+] = \theta_{HCA-OH_2^+} ([HCA-OH_2^+] + [HCA-OH]) \quad (3)$$

where θ is the fraction of the given species as determined by:

$$\theta_{X^-} = \frac{1}{1 + 10^{pKa_{(X^-)} - pH}} \quad (4)$$

and

$$\theta_{X-H} = \frac{1}{1 + 10^{pH - pKa_{(X-H)}}} \quad (5)$$

Inserting these functions into the expression for the equilibrium constant gives (eq 1):

$$K_d^{Ar-SO_2NH^-} = \frac{\theta_{Ar-SO_2NH^-} ([Ar-SO_2NH^-] + [Ar-SO_2NH_2]) \cdot \theta_{HCA-OH_2^+} ([HCA-OH_2^+] + [HCA-OH])}{[Ar-SO_2NH^- - Zn^{2+} - HCA][H_2O]} \quad (6)$$

Rearranging terms to give $K_d^{Ar-SO_2NH^-}$ as a function of known terms provides:

$$K_d^{Ar-SO_2NH^-} = \theta_{Ar-SO_2NH^-} \cdot \theta_{HCA-OH_2^+} \frac{([Ar-SO_2NH^-] + [Ar-SO_2NH_2])([HCA-OH_2^+] + [HCA-OH])}{[Ar-SO_2NH^- - Zn^{2+} - HCA][H_2O]} \quad (7)$$

Since the right-most factor of eq 7 is the observed equilibrium constant, this expression reduces to:

$$K_d^{Ar-SO_2NH^-} = \theta_{Ar-SO_2NH^-} \cdot \theta_{HCA-OH_2^+} \cdot K_{d,obs} \quad (8)$$

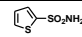
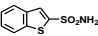
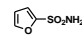
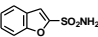
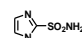
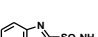

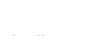

The observed enthalpy of dissociation (ΔH°_{obs}) contains contributions from three processes: i) dissociation of $Ar-SO_2NH^-$ from $HCA-Zn^{II}-OH_2^+$, ii) transfer of a proton from the buffer to $Ar-SO_2NH^-$, and iii) transfer of a proton from $HCA-Zn^{II}-OH_2^+$ to buffer. The observed enthalpy of dissociation is, thus:

$$\Delta H^\circ_{obs} = \Delta H^\circ_{Ar-SO_2NH^-} + \theta_{Ar-SO_2NH_2} (\Delta H^\circ_{ion,H_2PO_4^-} - \Delta H^\circ_{ion,Ar-SO_2NH_2}) + \theta_{HCA-Zn^{2+}-OH} (\Delta H^\circ_{ion,HCA-Zn^{2+}-OH_2^+} - \Delta H^\circ_{ion,H_2PO_4^-}) \quad (9)$$

To account for these three processes, we calculate the fraction of $Ar-SO_2NH^-$ and $HCA-Zn^{II}-OH_2^+$ that exchange protons with the buffer, and estimate the enthalpy of each process from the enthalpies of ionization of $Ar-SO_2NH^-$, $HCA-Zn^{II}-OH_2^+$, and $H_2PO_4^-$ (7-9). Rearranging eq 9 to provide the desired enthalpy ($\Delta H^\circ_{ArSO_2NH^-}$) as a function of known terms gives:

$$\Delta H^\circ_{Ar-SO_2NH^-} = \Delta H^\circ_{obs} - (1 - \theta_{Ar-SO_2NH^-}) (\Delta H^\circ_{ion,H_2PO_4^-} - \Delta H^\circ_{ion,Ar-SO_2NH_2}) - (1 - \theta_{HCA-Zn^{2+}-OH_2^+}) (\Delta H^\circ_{ion,HCA-Zn^{2+}-OH_2^+} - \Delta H^\circ_{ion,H_2PO_4^-}) \quad (10)$$

Table S3. Thermodynamic binding parameters for the binding of sulfonamides to HCA, corrected for the effects of ligand pK_a upon binding

| | | pK_a^a | ΔH_{ion}^b | $K_d^{ArSO_2NH^-}$ | $\Delta G^\circ_{ArSO_2NH^-}$ | $\Delta H^\circ_{ArSO_2NH^-}$ | $-T\Delta S^\circ_{ArSO_2NH^-}$ |
|------------|---|----------|---------------------------|--------------------|-------------------------------|-------------------------------|---------------------------------|
| | Compound | | (kcal mol ⁻¹) | (nM) | (kcal mol ⁻¹) | (kcal mol ⁻¹) | (kcal mol ⁻¹) |
| T |  | 9.6 | 8.4 ^c | 0.5 ± 0.1 | 12.7 ± 0.1 | 12.0 ± 0.1 | 0.7 ± 0.1 |
| BT |  | 9.2 | 8.1 ^c | 0.01 ± 0.003 | 14.9 ± 0.2 | 14.8 ± 0.4 | 0.1 ± 0.4 |
| F |  | 9.3 | 8.2 | 0.4 ± 0.01 | 12.8 ± 0.1 | 16.0 ± 0.4 | -3.2 ± 0.4 |
| BF |  | 8.9 | 7.9 | 0.02 ± 0.01 | 14.7 ± 0.1 | 17.4 ± 0.4 | -2.7 ± 0.4 |
| I |  | 8.8 | 7.8 ^c | 70 ± 20 | 9.8 ± 0.2 | 5.3 ± 0.4 | 4.5 ± 0.4 |
| BI |  | 8.3 | 7.6 ^c | 10 ± 1 | 10.9 ± 0.1 | 9.5 ± 0.1 | 1.4 ± 0.1 |
| TA |  | 8.4 | 7.7 | 1.2 ± 0.2 | 12.2 ± 0.1 | 13.4 ± 0.1 | -1.2 ± 0.1 |
| BTA |  | 8.1 | 7.4 | 0.06 ± 0.03 | 13.9 ± 0.3 | 16.2 ± 0.5 | -2.3 ± 0.6 |
| HBT |  | 9.8 | 8.5 | 0.02 ± 0.03 | 14.7 ± 0.1 | 14.4 ± 0.1 | 0.3 ± 0.1 |

^aMeasured by UV-spectroscopy as described above. ^bMeasured by ITC as described above. ^cEstimated using a linear relationship between reported values of pK_a and enthalpy of ionization of known sulfonamides (6). ^dCalculated using equation (8). Errors were estimated by propagating the errors from each of the parameters in equations (10). ^eCalculated using equation 4. Errors were estimated by propagating the errors from each parameter in equation 4 (excluding pK_a and $\Delta H^\circ_{ion,buffer}$). ^fErrors were estimated by propagating errors in $K_d^{ArSO_2NH^-}$ and $\Delta H^\circ_{ArSO_2NH^-}$.

Measurement of ΔG°_{ow} and ΔH°_{ow} of the ligands. *Shake-flask method:* We measured the equilibrium constant for partitioning between buffer (aqueous sodium phosphate, 10 mM, pH = 7.60 ± 0.03) and *n*-octanol using the shake-flask method. Briefly, ligands were dissolved in mutually saturated buffer (monocyclic compounds) or octanol (bicyclic compounds) at a concentration of $\sim 250 \mu\text{M}$. Aliquots of the ligand solution ($10.00 \pm 0.08 \text{ mL}$) and of the opposite phase ($10.00 \pm 0.08 \text{ mL}$) were combined in a 20 mL vial with a septum cap. After vigorous shaking for 18 hours using a “wrist-action” shaker, an aliquot of the aqueous phase was removed by syringe and the concentration of the ligand in that phase was analyzed by quantitative high pressure liquid chromatography or UV-visible spectroscopy. Values of ΔG°_{ow} represent the average of 5 – 7 experiments and the uncertainties show one standard deviation.

Solution Calorimetry: Solid sample of the ligand (5-10 mg) was placed in a glass ampoule, which was sealed with wax. The ampoule was placed in the calorimeter cell, which contained 100.0 mL of mutually pre-saturated octanol or buffered (10 mM phosphate, pH = 7.60) water. The cell was cooled to $\sim 297 \text{ K}$ prior to introduction into the heat sink (TAMIII, TA Instruments), which comprised an oil bath that was maintained thermostatically at 298 K. Upon introduction into the heat sink, heat transferred from the cell to the sink was recorded by the instrument. Experiments were conducted while the temperature of the cell equilibrated with the heat sink: two heat pulses were used to calibrate the heat capacity of the cell (1 J, 5 mW, 200 sec each), one before and one after the dissolution the sample. In each

experiment: the first calibration was performed when the temperature of the cell was ~250 mK below the temperature of the sink; the break was performed when the of the cell was < ~200 mK below the sink; and the second calibration was preformed when the of the cell was ~130 mK below the sink. Since the calibrations were of known power and time (i.e., heat = $q = p \cdot t$), the heat capacity of the cell is estimated by:

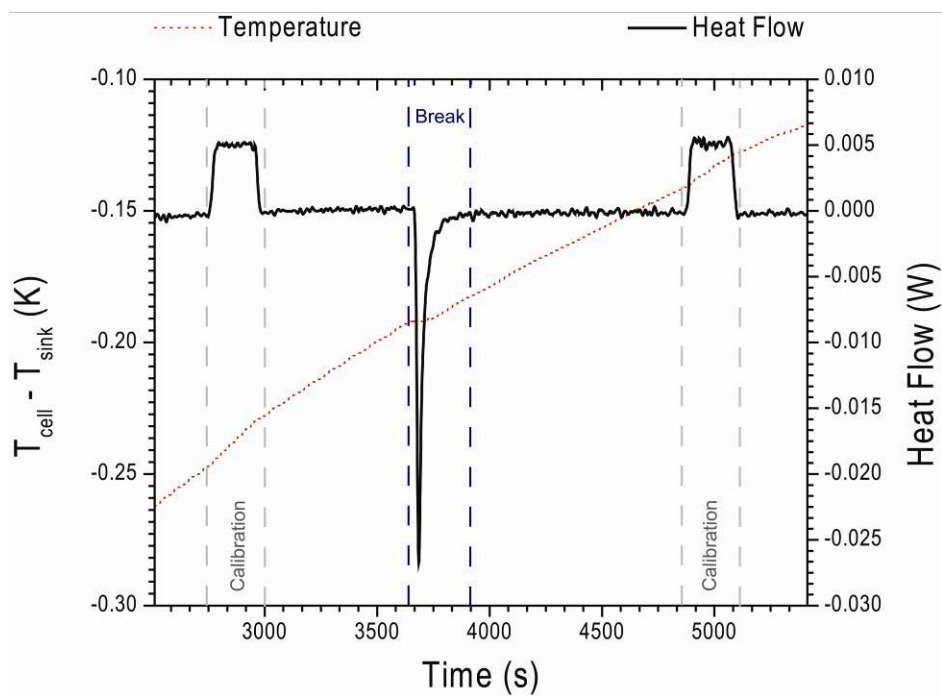
$$C_p = q_{\text{calibration}} / \Delta T \quad (11)$$

With a known heat capacity of the cell, the heat of the dissolution reaction is calculated by the temperature change for dissolution. To determine the proper endpoints for the dissolution experiment, the raw temperature data (K) were converted to heat flow (W) from the cell to the sink, using the SolCal software. This function clearly showed the return of the heat flow to baseline following the break of the ampoule (Figure S1). Each experiment was repeated 5-7 times, and following each experiment, the cell of the calorimeter was removed and examined for undissolved compound. For the ligands that appear in Figure 2 (**TA**, **BTA**, **I**, and **BI**), no solid sample remained. The other ligands, however, were not soluble enough to provide a measurable heat of dissolution in both water and octanol, and in each case solid sample remained in the cell of the calorimeter after the experiment.

The observed enthalpy of dissolution ($\Delta H^{\circ}_{\text{dissolution,obs}}$) for **TA**, **BTA**, **I**, and **BI** were determined by:

$$\Delta H^{\circ}_{\text{dissolution,obs}} = q_{\text{break}} / \text{moles of ligand} \quad (12)$$

Figure S2. Plots of the representative temperature (dashed red line) and heat flow (solid black line) data for the calibrations and dissolution of **BTA** into octanol.



Correction of the thermodynamic parameters of dissolution in to buffer for ionization of the sulfonamide. Since the observed equilibrium constant for partitioning of Ar-SO₂NH₂ between water and octanol ($K_{ow,obs}$) and the enthalpy of dissolution of Ar-SO₂NH₂ in buffer ($\Delta H^{\circ}_{dissolution,obs}$) depend on the ionization of this the ligand in the aqueous phase, we corrected the observed parameters using the following analysis. For the partitioning experiment, we assumed that Ar-SO₂NH₂ in the octanol phase was completely unionized and derived equations that accounted for the ionization of the sulfonamide in the aqueous phase (10 mM NaH₂PO₄, pH = 7.6). The desired equilibrium constant for partitioning from octanol to buffer was:

$$K_{ow}^{Ar-SO_2NH_2} = \frac{[Ar-SO_2NH_2]_w}{[Ar-SO_2NH_2]_o} \quad (13)$$

In the aqueous phase, the sulfonamide donates a proton to HPO₄²⁻ as described by:

$$K_a^{Ar-SO_2NH_2} = \frac{[Ar-SO_2NH^-][H^+]}{[Ar-SO_2NH_2]} \quad (14)$$

The observed equilibrium expression is thus:

$$K_{ow,obs} = \frac{\theta_{Ar-SO_2NH_2} ([Ar-SO_2NH_2]_w + [Ar-SO_2NH^-]_w)}{[Ar-SO_2NH_2]_o} \quad (15)$$

The right-most factor in eq 15 is the observed equilibrium constant for partitioning and the desired equilibrium constant is:

$$K_{ow,Ar-SO_2NH_2} = \theta_{Ar-SO_2NH_2} \cdot K_{ow,obs} \quad (16)$$

The observed enthalpy of dissolution of ligands in octanol is that of the Ar-SO₂NH₂, since we assume that there is no ionization equilibrium in that phase:

$$\Delta H^\circ_{o,obs} = \Delta H^\circ_{o,Ar-SO_2NH_2} \quad (17)$$

The dissolution of Ar-SO₂NH₂ in aqueous buffer, however, has contributions from dissolving Ar-SO₂NH₂ and from proton transfer described above. Although unexpected dimerization of the ligand in buffer could also contribute to the observed enthalpy of dissolution, ITC experiments in which we titrated the ligands into buffer (at concentrations of the ligand representative of the final concentrations of the ligand in the solution calorimetry experiment) showed no concentration dependence of the heat of dilution of the ligand. We thus eliminated contributions from ligand self-association as a source of enthalpy in the dissolution experiments. The observed enthalpy of dissolution of the sulfonamide ligands in buffer was thus modeled as:

$$\Delta H^\circ_{w,obs} = \Delta H^\circ_{w,Ar-SO_2NH_2} + \theta_{Ar-SO_2NH^-} (H^\circ_{ion,Ar-SO_2NH_2} - \Delta H^\circ_{ion,H_2PO_4^-}) \quad (18)$$

Rearranging terms in eq 18 gives the desired enthalpy of dissolution:

$$\Delta H^\circ_{w,Ar-SO_2NH_2} = \Delta H^\circ_{w,obs} - \theta_{Ar-SO_2NH^-} (H^\circ_{ion,Ar-SO_2NH_2} - \Delta H^\circ_{ion,H_2PO_4^-}) \quad (19)$$

The differences in values of dissolution of a ligand into water ($\Delta H^\circ_{w,Ar-SO_2NH_2}$) and octanol ($\Delta H^\circ_{o,Ar-SO_2NH_2}$) provided the values for $\Delta H^\circ_{ow,Ar-SO_2NH_2}$.

$$\Delta H^{\circ}_{ow,Ar-SO_2NH_2} = \Delta H^{\circ}_{w,Ar-SO_2NH_2} - \Delta H^{\circ}_{o,Ar-SO_2NH_2} \quad (20)$$

Using the values of $\Delta G^{\circ}_{ow,Ar-SO_2NH_2}$ estimated from $K_{ow,Ar-SO_2NH_2}$, and $\Delta H^{\circ}_{ow,Ar-SO_2NH_2}$ provides the entropy of partitioning by Gibbs equation:

$$\Delta G^{\circ}_{ow,Ar-SO_2NH_2} = \Delta H^{\circ}_{ow,Ar-SO_2NH_2} - T\Delta S^{\circ}_{ow,Ar-SO_2NH_2} \quad (21)$$

Estimation of the thermodynamic parameters for the benzo group. The thermodynamic parameters for the dissociation of the benzo substituent from the active site HCA (i.e., the parameter that describes the process of benzo extension in the active site) were calculated using:

$$\Delta J^{\circ}_{dissociation,benzo} = \Delta J^{\circ}_{dissociation,bicyclic-SO_2NH_2} - \Delta J^{\circ}_{dissociation,monocyclic-SO_2NH_2} \quad (22)$$

where $J = G, H$ or S . The thermodynamic parameters for partitioning of the benzo substituent from octanol to water were calculated using:

$$\Delta J^{\circ}_{ow,benzo} = \Delta J^{\circ}_{ow,bicyclic-SO_2NH_2} - \Delta J^{\circ}_{ow,monocyclic-SO_2NH_2} \quad (23)$$

Since the contribution to the observed thermodynamics of dissociation or partitioning are corrected for proton exchange with buffer (values on the right side of equations 22 and 23), and since the benzo group itself does not have protons that exchange with buffer, the values of $\Delta J^{\circ}_{dissociation,benzo}$ and $\Delta J^{\circ}_{ow,benzo}$, can be compared—as they are in Figure 2B—in a scheme that is independent of differences in the pK_a of the monocyclic and bicyclic ligands.

Protein Crystallization. Monoclinic crystals of HCA were grown by hanging drop diffusion following the method of McKenna and coworkers (10). Briefly, drops of crystallization medium were prepared by combining a solution of HCA (2 μ L, 100 μ M – 2 mM) in Tris-sulfate (100 mM, pH = 8.0) with a solution of sodium citrate/Tris-hydrogen chloride (2 μ M, 1.14 M, 100 mM) on a glass slide, which was subsequently sealed over a well containing sodium citrate/Tris-hydrogen chloride (1.0 mL, 1.14 M, 100 mM). As the drops equilibrated with the well solution by vapor diffusion, crystals of HCA grew over a period of two days to one month. Final sizes of the crystals varied from 100 μ m x 70 μ m x 50 μ m to 1 mm x 0.7 mm x 0.5 mm. The crystals were left undisturbed until needed for soaking experiments.

Ligand Soaking Experiments. In order to prohibit the dissolution of crystals upon transfer of them to solutions that contained ligand, we prepared solutions of ligands in sodium citrate at a higher concentration than the mother liquor of the crystals (1.34 M sodium citrate, 100 mM Tris-hydrochloride, pH = 7.6). We also, avoided, when possible, the use of DMSO in the soaking solutions (i.e., solid samples of the ligands were used to saturate the soaking solutions). Typically, small crystals (100 μ m x 70 μ m x 50 μ m) were selected for soaking experiments. Crystals were transferred into saturated solutions of ligand in sodium citrate/Tris-HCl and left to soak at 4° C for two days to one week.

X-ray crystallography. Crystals were harvested using a Nylon loop, frozen in liquid nitrogen without the use of cryoprotectant. All data were collected at Brookhaven National Laboratory on the ADSC Quantum Q315 CCD detector at the National Synchrotron Light Source at (X25) in collaboration with the Mail-Program, Brookhaven National Laboratory (11). Reflections were indexed and integrated using HKL2000, and scaled using SCALEPACK (12).

Solution of Crystal Structures. Diffraction data were analyzed using the CCP4i suite of crystallography software (13). Phases were determined by molecular replacement with a previously reported structure of native HCA II (PDBID: 2ILI) less atoms of water and zinc. In each case, presence of the ligand in the active site was obvious in the weighted difference map. Molecules of water and alternate conformations were added to peaks in the difference map that were $> 5\sigma$, with intervening cycles of 5 – 10 rounds of restrained refinement.

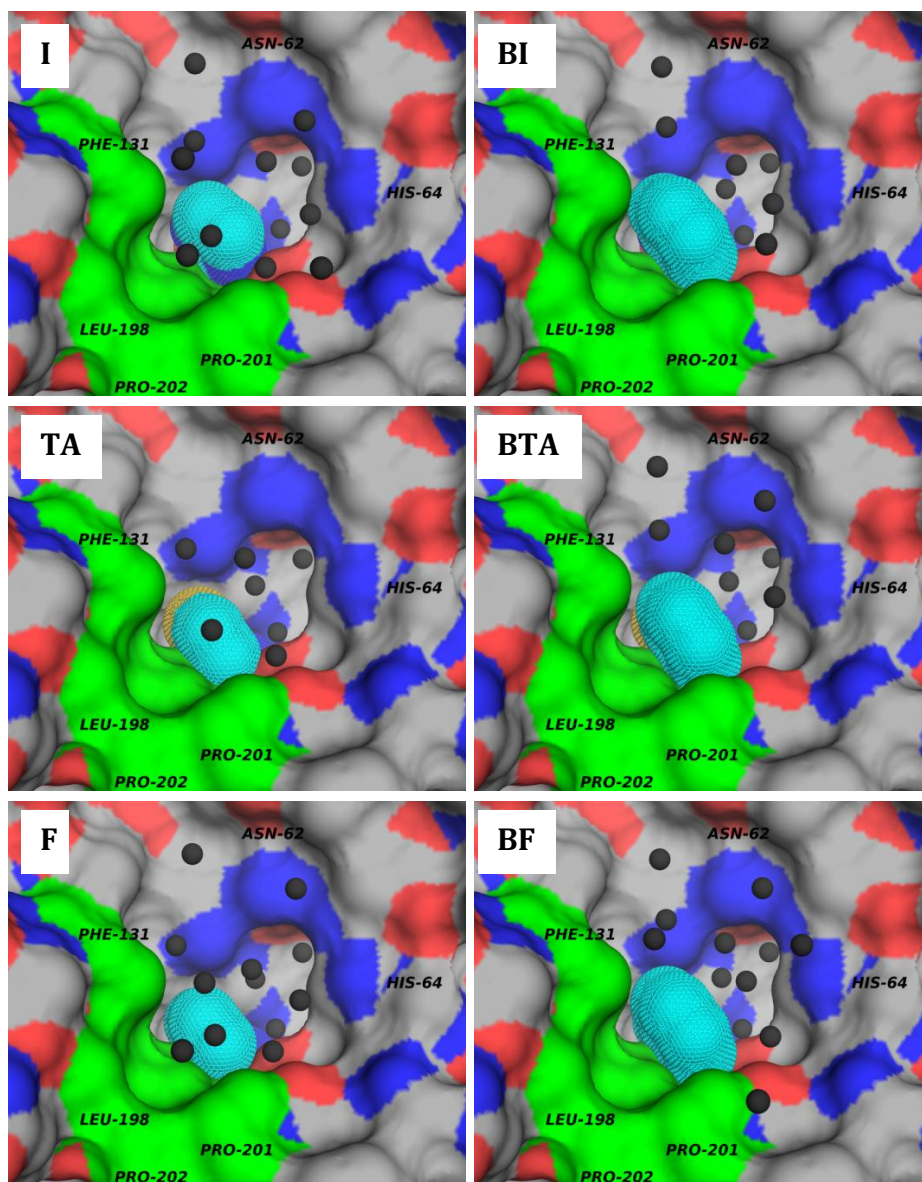
Table S4. Crystallography data for the ligand-HCA complexes.

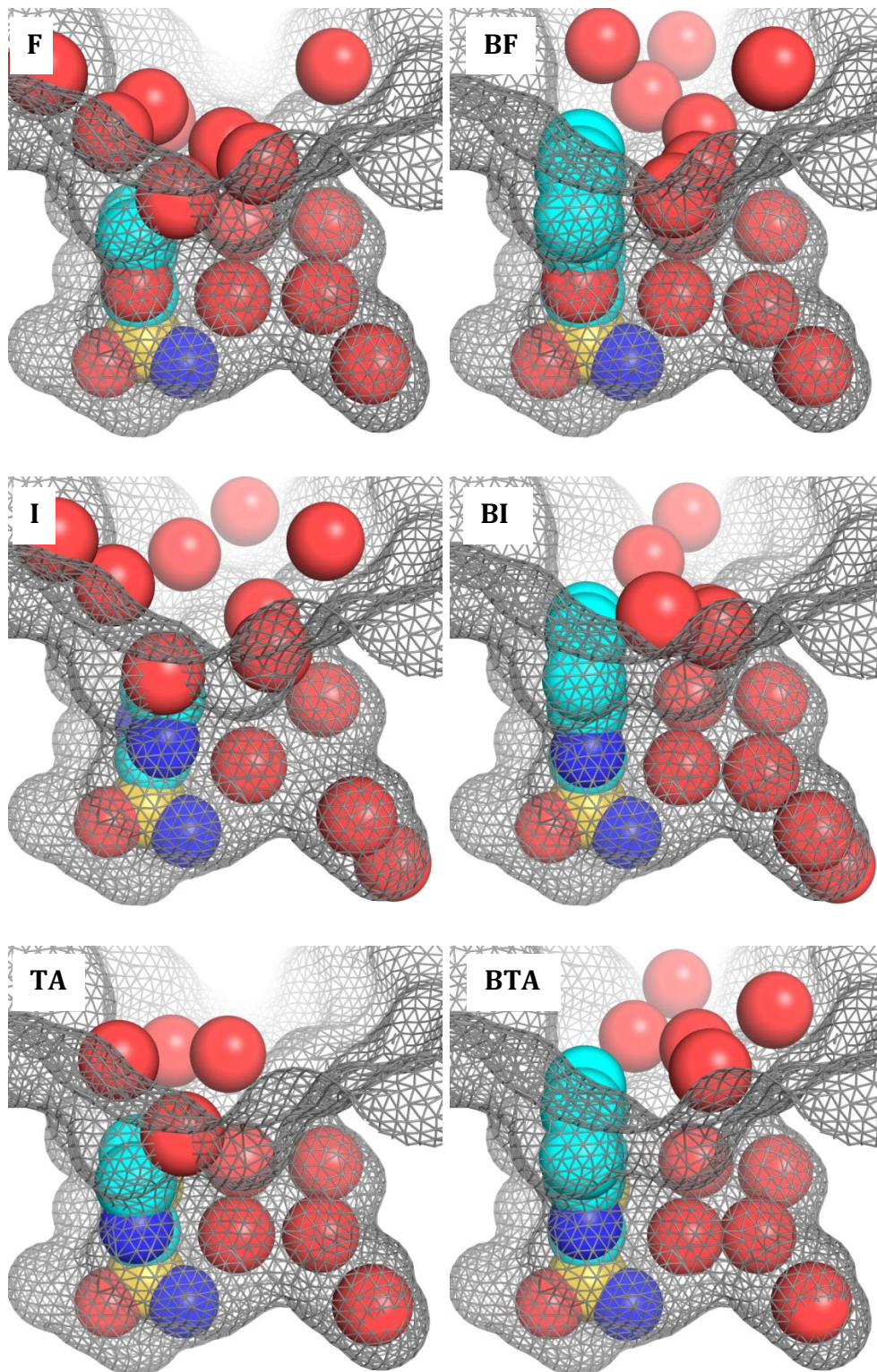
| | F-HCA | BF-HCA | T-HCA | BT-HCA | TA-HCA | BTA-HCA | I-HCA | BI-HCA |
|--|------------------|------------------|------------------|------------------|------------------|------------------|------------------|------------------|
| Unit cell^a a, Å | 42.38 | 42.37 | 41.99 | 42.22 | 42.13 | 42.76 | 42.30 | 42.13 |
| b | 41.43 | 41.40 | 40.96 | 41.21 | 41.09 | 41.92 | 41.44 | 41.45 |
| c | 72.50 | 72.47 | 71.64 | 72.09 | 71.96 | 72.57 | 72.60 | 72.52 |
| α ° | 90.00 | 90.00 | 90.00 | 90.00 | 90.00 | 90.00 | 90.00 | 90.00 |
| β | 104.66 | 104.69 | 104.27 | 104.61 | 104.32 | 102.81 | 104.66 | 104.53 |
| γ | 90.00 | 90.00 | 90.00 | 90.00 | 90.00 | 90.00 | 90.00 | 90.00 |
| Reflection Statistics^{b,c} | | | | | | | | |
| Hi-Resolution bin | 1.53 – 1.50 | 1.27 – 1.25 | 2.01 – 1.98 | 1.42 – 1.40 | 1.89 – 1.86 | 1.81 – 1.75 | 1.63 – 1.60 | 1.63 – 1.60 |
| Unique Reflections (#) | 36000 (1024) | 61155 (1391) | 16439 (712) | 41672 (997) | 19847 (814) | 23728 (1615) | 31878 (1428) | 29906 (1112) |
| Completeness (%) | 91.7 (51.7) | 91.0 (41.8) | 97.0 (83.5) | 87.6 (42.0) | 96.7 (79.4) | 93.1 (100) | 98.6 (90.4) | 92.8 (70.1) |
| R_{merge} (%) | 0.044 (0.191) | 0.051 (0.335) | 0.083 (0.388) | 0.052 (0.467) | 0.079 (0.505) | 0.057 (0.574) | 0.049 (0.358) | 0.058 (0.391) |
| Redundancy | 4.9 (2.7) | 5.3 (2.6) | 6.7 (4.2) | 6.1 (5.1) | 5.1 (3.4) | 6.4 (3.6) | 6.8 (4.7) | 6.7 (5.4) |
| Net I/σ (avg) | 16.7 | 17.2 | 10.4 | 16.9 | 9.7 | 18.1 | 19.2 | 16.2 |
| Refinement Statistics^c | | | | | | | | |
| Hi-Resolution bin | 1.54 – 1.50 | 1.28 – 1.25 | 2.02 – 1.97 | 1.44 – 1.40 | 1.90 – 1.86 | 1.80 – 1.75 | 1.64 – 1.60 | 1.64 – 1.60 |
| Completeness (%) | 91.6 (53.6) | 90.9 (44.6) | 97.1 (91.0) | 87.5 (44.0) | 96.7 (86.5) | 96.7 (100) | 98.6 (92.5) | 92.8 (75.4) |
| R_{obs} | 0.151 | 0.158 | 0.176 | 0.167 | 0.180 | 0.180 | 0.159 | 0.161 |
| R_{work} | 0.155 (0.182) | 0.157 (0.292) | 0.173 (0.247) | 0.165 (0.321) | 0.178 (0.294) | 0.178 (0.277) | 0.157 (0.354) | 0.159 (0.313) |
| R_{free} | 0.191 (0.234) | 0.181 (0.327) | 0.223 (0.355) | 0.203 (0.378) | 0.219 (0.407) | 0.219 (0.299) | 0.193 (0.387) | 0.199 (0.354) |
| B_{avg} | 12.65 | 12.82 | 22.76 | 14.72 | 22.67 | 22.67 | 14.94 | 14.38 |
| bonds^d (Å) | 0.028 | 0.029 | 0.022 | 0.028 | 0.024 | 0.025 | 0.027 | 0.027 |
| angles^e (°) | 2.402 | 2.64 | 2.192 | 2.566 | 2.224 | 2.25 | 2.299 | 2.245 |
| PDB ID | 3S75 | 3S71 | 3S78 | 3S74 | 3S77 | 3S73 | 3S76 | 3S72 |

^aAll crystals belonged to the P2₁ space group. ^bAll data were measured with $\lambda = 1.100$ Å at a low resolution limit of 50.00 Å. ^cValues in parentheses represent those for the highest resolution shell. ^dThe root-mean-square deviation of the bond lengths in the structure. ^eThe root-mean-square deviation of the bond angles in the structure.

Figure S3. Crystallographically defined molecules of water in the active site of HCA.

A) Atoms of the protein appear as colored van der Waals surfaces with green representing the carbon atoms of the hydrophobic shelf, red representing atoms of oxygen, and blue indicating atoms of nitrogen. The ligand atoms appear as spheres with an overlaid mesh that represents the van der Waals surfaces. Gray spheres represent molecules of water that appear in the crystal structures. Each image is labeled with the corresponding symbol for the ligand. B) As in Figure 4B, the binding pocket of HCA appears as a mesh surface representation. Atoms of the ligands and crystallographically determined molecules of water appear as sphere representations.





WaterMap Calculations. The WaterMap method computes water properties (location, occupancy, enthalpy, entropy, and free energy) by combining molecular dynamics, solvent clustering, and statistical thermodynamic analysis. First, a 9 ns explicit-solvent molecular dynamics simulation of the protein-ligand complex is run in order to sample the energies and configurations of water molecules around the active site. To ensure convergence of the water free energies around a protein-ligand complex conformation of interest, the coordinates of the protein and ligand are restrained with a $5.0 \text{ kcal mol}^{-1} \text{ \AA}^{-2}$ harmonic potential applied to the crystallographic positions of the heavy atoms. Waters from approximately 2000 equally spaced frames from the molecular dynamics simulation are then spatially clustered to form hydration sites and the thermodynamic properties of those sites are computed.

The enthalpy is computed as the average non-bonded molecular mechanics interaction energies of the waters in the hydration site with the rest of the system. The entropy is computed by numerically integrating a local expansion of spatial and orientational correlation functions, as described in the inhomogeneous fluid thermodynamics works by Lazaridis (14-15). The relevant thermodynamic quantities for this work are the difference in enthalpy, entropy, and free energy of the hydration sites for the structure with ligand before and after the benzo-extension.

To make an accurate comparison between the structures, we retained the 30 hydration sites closest to each ligand, which corresponds to a shell of approximately 10.0 \AA beyond the

ligand. The enthalpy, entropy, and free energy of these 30 sites were summed for each ligand and the relevant differences were taken (**BF-F** and **BT-T**). In the case of the **BT** ligand there was multiple occupancy in the crystal structure so separate calculations were performed on each state and the values were averaged. The computed thermodynamic quantities for each of the ligands, including the multiple two structures for **BT**, are shown in Table S5 below.

Table S5. WaterMap Results.^a

| | ΔH | $-T\Delta S$ | ΔG | $\frac{\Delta H_{\text{benzo}} - \Delta H_{\text{non-benzo}}}{\Delta H_{\text{non-benzo}}}$ | $\frac{(-T\Delta S_{\text{benzo}}) - (-T\Delta S_{\text{non-benzo}})}{(-T\Delta S_{\text{non-benzo}})}$ | $\frac{\Delta G_{\text{benzo}} - \Delta G_{\text{non-benzo}}}{\Delta G_{\text{non-benzo}}}$ |
|---------------------|------------|--------------|------------|---|---|---|
| F | 9.55 | 49.54 | 59.09 | | | |
| BF | 6.33 | 50.33 | 56.65 | -3.22 | 0.78 | -2.44 |
| T | 6.05 | 49.37 | 55.43 | | | |
| BT av | 3.22 | 49.02 | 52.24 | -2.83 | -0.36 | -3.19 |
| BT occ _a | 3.21 | 48.56 | 51.77 | | | |
| BT occ _b | 3.24 | 49.47 | 52.71 | | | |

^aAll values are reported in units of kcal mol⁻¹.

References

1. Burton RE, Oas TG, Fterke CA, & Hunt JA (2000) Novel disulfide engineering in human carbonic anhydrase II using the PAIRWISE side-chain geometry database. *Protein Sci* 9:776-785.
2. Khalifah RG, Strader DJ, Bryant SH, & Gibson SM (1977) Carbon-13 nuclear magnetic resonance probe of active-site ionizations in human carbonic anhydrase B. *Biochemistry* 16:2241-2247.
3. Maniara G, Rajamoorthi K, Rajan S, & Stockton GW (1998) Method Performance and Validation for Quantitative Analysis by 1H and 31P NMR Spectroscopy. Applications to Analytical Standards and Agricultural Chemicals. *Anal Chem* 70:4921-4928.
4. Tellinghuisen J (2005) Optimizing Experimental Parameters in Isothermal Titration Calorimetry. *J Phys Chem B* 109:20027-20035.
5. Wiseman T, Williston S, Brandts JF, & Lin L-N (1989) Rapid measurement of binding constants and heats of binding using a new titration calorimeter. *Anal Biochem* 179:131-137.
6. Krishnamurthy VM, *et al.* (2007) Thermodynamic parameters for the association of fluorinated benzenesulfonamides with bovine carbonic anhydrase II. *Chem Asian J* 2:94-105.
7. Silverman DN & Lindskog S (1988) The catalytic mechanism of carbonic anhydrase: implications of a rate-limiting protolysis of water. *Acc Chem Res* 21:30-36.

8. DiTusa CA, Christensen T, McCall KA, Fierke CA, & Toone EJ (2001) Thermodynamics of Metal Ion Binding. 1. Metal Ion Binding by Wild-Type Carbonic Anhydrase[†]. *Biochemistry* 40:5338-5344.
9. Goldberg RN, Kishore N, & Lennen RM (2002) Thermodynamic Quantities for the Ionization Reactions of Buffers. *J Phys Chem Ref Data* 31:231-370.
10. Fisher SZ, *et al.* (2007) Atomic Crystal and Molecular Dynamics Simulation Structures of Human Carbonic Anhydrase II: Insights into the Proton Transfer Mechanism^{†,‡}. *Biochemistry* 46:2930-2937.
11. Robinson H, Soares AS, Becker M, Sweet R, & Heroux A (2006) Mail-in crystallography program at Brookhaven National Laboratory's National Synchrotron Light Source. *Acta Crystallogr D* 62:1336-1339.
12. Otwinowski Z & Minor W (1997) [20] Processing of X-ray diffraction data collected in oscillation mode. ed Charles WC, Jr. (Academic Press), Vol Volume 276, pp 307-326.
13. Collaborative (1994) The CCP4 suite: programs for protein crystallography. *Acta Crystallogr D* 50:760-763.
14. Lazaridis T (1998) Inhomogeneous Fluid Approach to Solvation Thermodynamics. 2. Applications to Simple Fluids. *J Phys Chem B* 102:3542-3550.
15. Lazaridis T (1998) Inhomogeneous Fluid Approach to Solvation Thermodynamics. 1. Theory. *J Phys Chem B* 102:3531-3541.